Structure of Surfaces from Classical and Quantum Mechanical Rainbow Scattering of Fast Atoms

H. Winter, M. Busch, A. Schüller, J. Seifert, and S. Wethekam

[1] *Humboldt Universität zu Berlin, Institut für Physik, Brook-Taylor-Str. 6, 12489 Berlin, Germany*

winter@physik.hu-berlin.de

Abstract: The structure of clean and adsorbate covered surfaces as well as of ultrathin films can be investigated by grazing scattering of fast atoms from the surface. We present two recent experimental techniques which allow us to study the structure of ordered arrangements of surface atoms in detail. (1) rainbow scattering under axial surface channeling conditions, and (2) fast atom diffraction. Our examples demonstrate the attractive features of grazing fast atom scattering as a powerful analytical tool in studies on the structure of surfaces. We will concentrate our discussion on the structure of ultrathin silica films on a Mo(112) surface and of adsorbed oxygen atoms on a Fe(110) surface.

1. Introduction

Thin oxide films are widely used in a variety of applications ranging from electronic devices to catalysis [1]. Grown as ultrathin films on metal substrates, the problem of low conductivity of bulk oxides is avoided so that established surface science tools are applicable. An important oxide in advanced technology is silica (SiO_2) for which the preparation of ultrathin well-ordered films has been demonstrated on a Mo(112) surface [2, 3]. Despite considerable efforts in order to clear up the geometrical structure of this film by a number of different experimental and theoretical methods, the detailed structure of the silica film on Mo(112) is still a matter of debate [4]. Two conflicting models for the film structure are presently discussed:

(1) A honeycomb-like 2D-network model formed by corner-sharing SiO_4 tetrahedra [5, 6],

(2) a cluster model consisting of isolated SiO_4 tetrahedra where all oxygen atoms are bound to the molybdenum surface [4, 7 - 9].

In our work we have investigated with a new technique the structure of ultrathin silica films on Mo(112) based on grazing scattering of fast atoms along low indexed axial channels of surface atoms ("axial surface channeling" [10 – 12]. Under these conditions, the effective scattering potential has cylindrical symmetry with respect to individual strings formed by topmost surface atoms. The resulting corrugation of the potential leads to an out-of plane scattering where the maximum for the azimuthal angular deflection shows an intensity enhancement for scattered atoms, the so called collisional "rainbow" [13]. Rainbow scattering for fast atoms at surfaces can be used to obtain information on the corrugation of the interaction potential and, in particular, on the arrangement of atoms at the surface [24, 25]. We will demonstrate here that this method can be applied to study the structure of ultrathin silica films on Mo(112) and provides severe tests on structural models.

For sufficiently small angles of incidence and projectile energies, excitations of the solid are on such a low level that in combination with the high angular resolution achieved for grazing surface scattering of fast atoms, diffraction phenomena can be observed for the scattered particles [14 - 16]. Striking feature of Fast Atom Diffraction (FAD) under axial surface channeling is the presence of quantum scattering for matter waves with de Broglie wavelengths which are about three orders of magnitude smaller than typical periodicity lengths for ordered structures of surfaces. FAD can be considered as an additional tool to study surface structures with fast atomic beams which extends the regime of the established method of He atom scattering (HAS) at thermal energies [17] to keV energies. A major advantage for diffraction studies with fast atoms is the efficient detection by means of direct imaging so that complete diffraction patterns for FAD can be recorded in time scales of several seconds up to minutes. As a representative example we discuss studies on the positions of O adatoms on a Fe(110) surface.

2. Experiment

The preparation of the silica films and the scattering experiments were performed in an UHV chamber at a base pressure in the upper 10^{-11} mbar range. The Mo(112) surface was initially prepared by cycles of grazing sputtering with 25 keV Ar^+ ions and annealing at temperatures of about 1900 K for several minutes. Thereafter, no contaminations as carbon or oxygen could be detected within the sensitivity limit of our Auger electron spectroscopy setup (CLAM2 spectrometer, VG instruments) and sharp p(1x1) LEED patterns were observed with a SPALEED system (Omicron Nanotechnology). Deposition of silicon atoms was performed using an electron beam evaporator (EFM3, Omicron Nanotechnology) from a high purity silicon rod (GoodFellow). The evaporation rate amounted to about 0.25 monolayers (ML) per minute. Oxygen was dosed by backfilling the UHV chamber using a high precision leak valve.

Following the recipe given in [18], the monolayer silica films were prepared by deposition of 1.2 ML silicon at 900 K at a partial oxygen pressure of $5 \cdot 10^{-8}$ mbar on an oxygen covered Mo(112) surface. Annealing at about 1200 K in UHV leads to well ordered silica films showing sharp c(2x2) LEED patterns. The angular

distributions of scattered atoms were recorded with a position sensitive micro channel plate (MCP) detector (DLD40, Roentdek GmbH) with an active surface of 48 mm diameter positioned at a distance of 83cm behind the target.

3. Results

3.1 Classical rainbow scattering

In Fig. 1 we show a 2D intensity plot for scattering of 2 keV He atoms from the ultrathin silica film on Mo(112) along a low indexed axial channel. The intensity pattern reveals a circular shape owing to the axial symmetry for the scattering process with three intense peaks. The symmetrically two outer peaks located at the extreme of the azimuthal angular deflection can be ascribed to rainbow scattering in the interaction potential with a corrugation normal to the direction of the atomic strings.

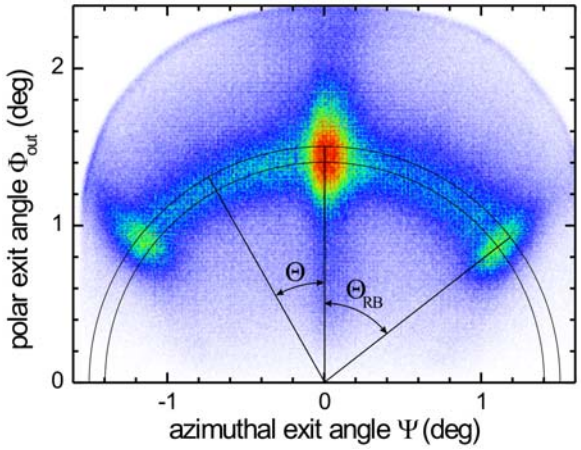

Fig. 1. 2D intensity pattern for scattering of 2 keV He atoms from ultrathin silica film on Mo(112) along $[\bar{1}\,\bar{1}\,1]$.

The relatively large rainbow angle points towards a considerable corrugation of the interaction potential along this axial channel. The intense peak in the middle stems primarily from scattering from flat parts of the equipotential plane within the axial channels giving rise to a focusing in forward direction ("glory effect").

For the analysis of angular distributions as shown in Fig. 1 we project the intensity within an annulus as drawn in the figure onto the scale of the deflection angle Θ. The solid curve in Fig. 2 presents a corresponding plot for the data shown in Fig. 3 with an intense peak at $\Theta = 0$ and the two rainbow peaks at $\Theta_{RB} \approx 50°$.

In order to test for the two conflicting structural models, we performed computer simulations of projectile trajectories based on classical mechanics. For these calculations, the projectile-surface interaction potentials are important. We have chosen here a superposition of inter-atomic pair potentials in the Thomas-Fermi approximation proposed by O'Connor and Biersack [19].

In the regime of axial surface channeling, the effective potential is obtained by an averaging of the individual pair potential over atomic strings. The trajectories can be derived then from the resulting two-dimensional continuum potential. Since contributions of electronic properties of atoms embedded into the electron gas in the selvedge of the surface as well as polarization effects are neglected here, uncertainties with respect to the positions of atoms have to be taken into account. Since the main issue of this work is focused on the comparison of two fairly different structural models, this uncertainty is hardly essential for the comparison of data on a relative scale. The intensity pattern as function of deflection angle Θ was derived from the number of trajectories which pass for a given interval of distances normal to axial channels a defined interval of deflection angles. Experimental and inherent broadenings via thermal lattice vibrations are taken into account by convolution of the calculated angular distributions with a Gaussian line shape.

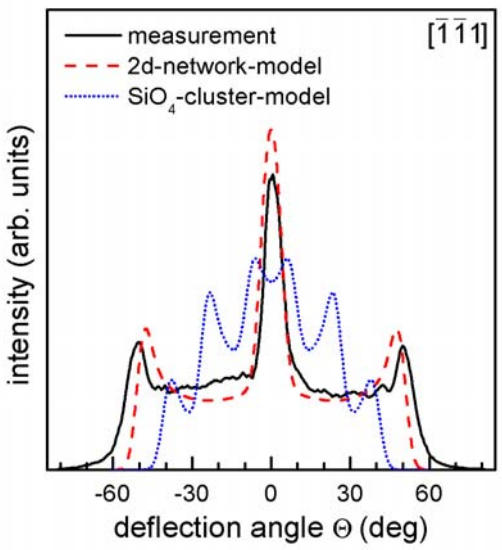

Fig. 2. Projected intensity as function of deflection angle Θ for scattering of 2 keV He atoms from silica film on Mo(112) along $[\bar{1}\,\bar{1}\,1]$ under $\Phi_{in} = 1.5°$.

In Fig. 3 we display projections of calculated classical trajectories into a plane normal to the $[\bar{1}\,\bar{1}\,1]$ direction. The thick solid curves denote sections of equi-potential curves for 0.5 eV, 1 eV, 2 eV, 4 eV, and 8 eV. The trajectories shown are calculated for scattering of 2 keV He atoms from the ultrathin silica film for the network (upper panels) and cluster model (lower panels). The enhancements in the spatial density of trajectories at the extremes of angular deflection give rise to rainbow peaks in the angular distributions. Note the substantial difference in the shape of the potential planes for the two different structural models.

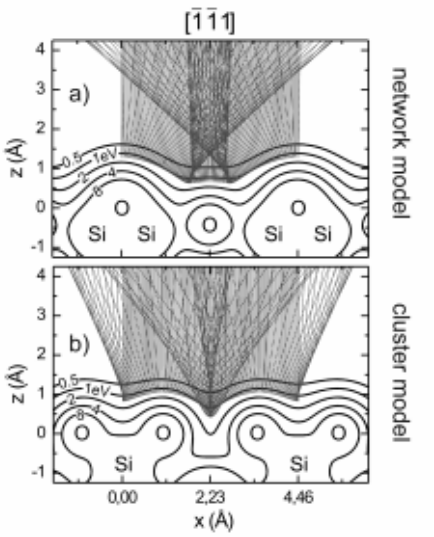

Fig. 3. Calculated trajectories in plane normal to $[\bar{1}\,\bar{1}\,1]$ axial channel for 2 keV He and $\Phi_{in} = 1.5°$.

The comparison of our calculations with the experiments is given for the 2D-network model (dashed curves) and for the cluster model (dotted curves) in Fig. 2. For scattering along the $[\bar{1}\,\bar{1}\,1]$ azimuth, the cluster model reveals several rainbow peaks (see also panel b of Fig. 3), in conflict with the experiment.

For calculations based on the 2D-network model (dashed curve in Fig. 2), however, we find good agreement for the positions of the rainbow peaks and the overall shape of the angular distributions. Aside from the positions of the two rainbow peaks also the intensity for small deflection angles is fairly well reproduced.

3.1 Fast Atom Diffraction (FAD)

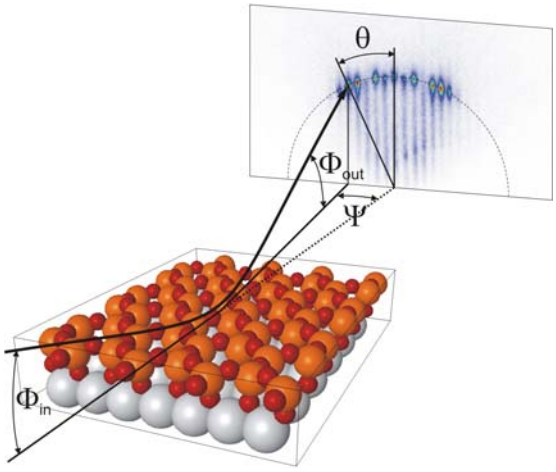

Fig. 4. Sketch of collision geometry for Fast Atom Diffraction (FAD).

In Fig. 4 we show a sketch of the scattering geometry for FAD and an experimental diffraction pattern for 2 keV ^{3}He atoms scattered from the silica film on Mo(112) under $\Phi_{in} = 0.9°$ along the axial channel. The resulting diffraction pattern is indeed closely related to rainbow scattering. The "grating" for FAD is the arrangement of axial strings (periodicity of interaction potential normal to atomic strings) so that the separation of diffraction spots provides information on the width of axial channels, i.e. the periodicity length of the interaction potential. For a length d, the Bragg condition for constructive interference reads $n\,\lambda_{dB} = d\,\sin\Psi$ with n being the diffraction order and Ψ the azimuthal scattering angle. Since $\lambda_{dB} << d$, Ψ and the angular splittings between adjacent diffraction peaks $\Delta\Psi$ are small (typically 0.1°). However, for coherent quantum scattering under grazing incidence the effects for broadening of the scattered beam owing to thermal vibrations of lattice atoms is substantially reduced [20] and the angular resolution is sufficiently high in order to resolve diffraction peaks.

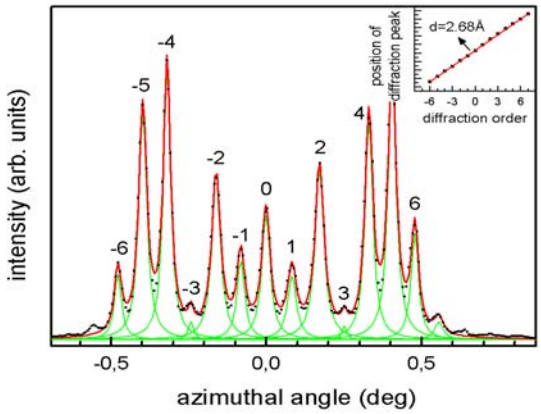

Fig. 5. Projection of intensity for scattered projectiles on azimuthal angle Ψ for scattering of 2 keV ^{3}He atoms from silica film on Mo(112) under $\Phi_{in} = 0.9°$. Solid curves: best fits to Lorentzian line shapes.

In Fig. 5 we show the projection of the intensities of the diffraction pattern shown in Fig. 4 and in the insert a plot of the azimuthal exit angle for the positions of the diffraction spots of order n which reveals the expected linear dependence $\Psi \approx n\,\lambda_{dB} / d$. We obtain from a best fit to the data d = 2.68 Å which is in good accord with the width of this channel for the Mo(112) substrate of 2.73 Å. Since for the 2D-network model each second string in the topmost layer has the double line density of O atoms, the resulting periodicity of the interaction potential is the same as for the substrate, in agreement with the experiment. For the cluster model, adjacent strings have the same line density so that the periodicity length would be reduced by a factor of two which is not observed in the diffraction spectra. Therefore also the diffraction pattern of fast atoms is in favour the 2D network model. Since the Si atoms in the film layer affect the overall potential, a more detailed analysis of

these preliminary data has to be performed, before definite conclusions can be drawn on this issue.

In order to demonstrate the power of FAD for studies on the structure of surfaces in more detail, we discuss recent work [21] on the adsorption of oxygen on a Fe(110) surface. For an O_2 dose of 2 Langmuir (1 L = 1 Langmuir = 1.33 10^{-6} mbar sec) and subsequent annealing at 770 K for about 10 minutes, one observes via LEED a well defined c(2x2)O/Fe(110) phase. In Fig. 6 we show FAD diffraction patterns for scattering of 0.50 keV (upper panel), 0.70 keV (middle panel), and 1.10 keV ^{3}He atoms (lower panel) at $\Phi_{in} = 0.85°$, where spots up to order n = 4 can be identified. From the angular splittings $\Delta\Psi$ we deduce a width of 2.87 Å for the $[\bar{1}\,\bar{1}\,1]$ channel which is in good agreement with 2.86 Å for a structural model where the O atoms occupy four-fold hollow site positions on the Fe(110) substrate.

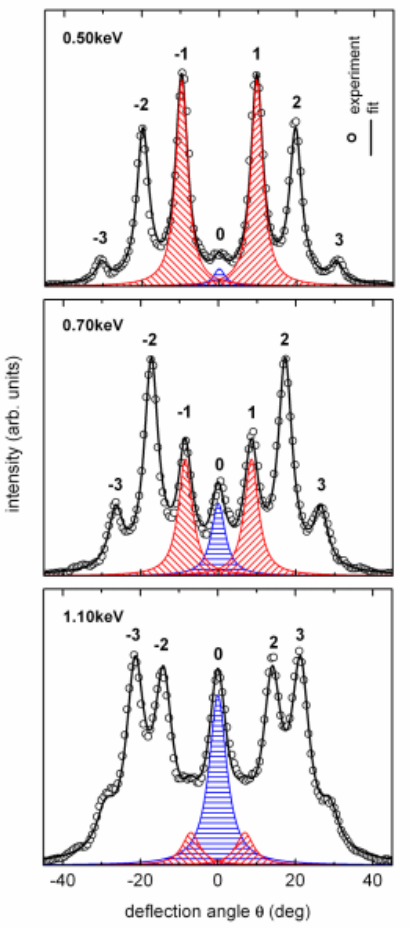

Fig. 6. Projection of intensity with respect to deflection angle Θ for scattering of 0.5 keV (upper panel), 0.7 keV (middle panel), and 1.1 keV ^{3}He atoms (lower panel) from c(2x2)O/Fe(110) under $\Phi_{in} = 0.85°$. Solid curves: best fits to Lorentzian lineshapes.

A closer inspection of the diffraction patterns in Fig. 6 reveals a change of relative intensities for different diffraction orders with energy. This variation of intensities depends strongly on the corrugation of the He surface interaction potential. Based on the approximation for scattering from a hard wall potential [22, 23], one can deduce the corrugation Δz of the potential surface as function of $E_\perp = E \sin^2\Phi_{in}$. In the upper panel of Fig. 7 we have plotted relative intensities for the zeroth and first order peaks as function of the de Broglie wavelength for the motion of atoms normal with respect to the surface plane $\lambda_{dB\perp} = h / (2\,M\,E_\perp)^{1/2}$. The solid curves are best fits to the data with Bessel functions by intensities $I_n \sim [J_n(2\pi\,\Delta z/\,\lambda_{dB\perp})]^2$ for n = 0 and 1 where Δz as fit parameter is assumed to depend linearly on $E_\perp$. In the lower panel of Fig. 7 we have plotted the resulting dependence for Δz revealing a corrugation in the range from 0.2 Å to about 0.25 Å.

The corrugation Δz is very sensitive to the positions of O atoms which are located at a height h atop axial strings of Fe substrate atoms. Based on individual He – O and He – Fe interatomic potentials derived from HF wave functions, we have calculated the corrugation Δz for this channel as function of potential energies $E_\perp$ for different heights h.

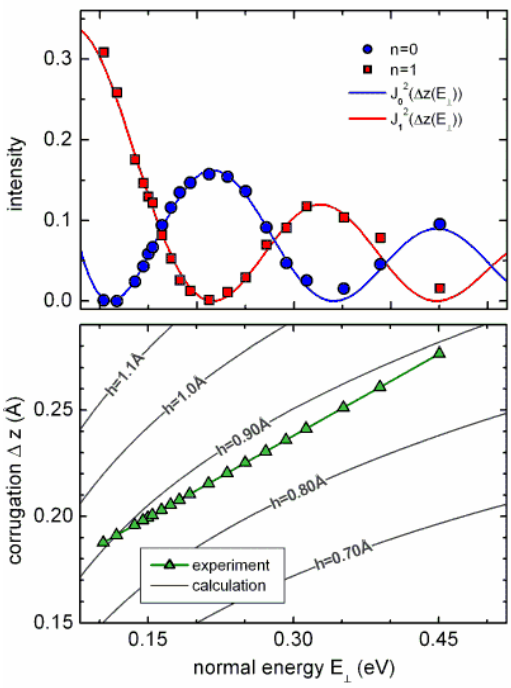

Fig. 7. Upper panel: Intensity of diffraction spots of order n = 0 (full circles) and n =1 (squares). Solid curves represent best fit to data by J_n^2 (for details see text).

Lower panel: Corrugation Δz as function of normal energy $E_\perp$. Full triangles: analysis of experiment in terms of hard wall approximation; solid curves: corrugation of potential for different distances h of oxygen atoms to Fe substrate.

We find best agreement with the linear dependence $\Delta z(E_\perp)$ deduced from the intensity modulations for n = 0 and 1, if h = 0.87 Å is chosen. Since our analysis is performed in the hard wall approximation, h has to be corrected slightly in a more realistic evaluation of data. Such an analysis for all accessible orders of diffraction patterns for four low indexed channels finally leads to h = (0.9 ± 0.2) Å [24] which is consistent with recent DFT calculations for this system [25]. A similar analysis of data is in preparation for the SiO2/Mo(112) system discussed above.

The assistance of K. Maass, G. Lindenberg, and M. Reinhardt in performing the experiments is gratefully acknowledged. This work was supported by the DFG in Sonderforschungsbereich 546 "Struktur, Dynamik und Reaktivität von Übergangsmetalloxid-Aggregaten".

References

[1] H. J. Freund, Faraday Discussions 114 (1999) 1

[2] T. Schroeder, M. Adelt, B. Richter, M. Naschitzki, M. Bäumer and H.-J. Freund, Surf. Rev. Lett. 7 (2000) 7

[3] T. Schroeder, J.B. Giorgi, M. Bäumer and H.-J. Freund, Phys. Rev. B 66 (2002) 165422

[4] M. S. Chen and D. W. Goodman, J. Phys.: Cond. Matter 20 (2008) 264013

[5] J. Weissenrieder, S. Kaya, J.-L. Lu, H.-J. Gao, S. Shaikhutdinov, H.-J. Freund, M.M. Sierka, T.K. Todorova and J. Sauer, Phys. Rev. Lett. 95 (2005) 076103

[6] S. Kaya, M. Baron, D. Stacchiola, J. Weissenrieder, S. Shaikhutdinov, T.K. Todorova, M. Sierka, J. Sauer, H.-J. Freund, Surf. Sci. 601 (2007) 4849

[7] M. Chen, A.K. Santra and D.W. Goodman, Phys. Rev. B 69 (2004) 155404

[8] M. Chen and D.W. Goodman, Surf. Sci. 601 (2007) 591

[9] I.N. Yakovkin, Surf. Rev. Lett. 12 (2005) 449

[10] D. Gemmell, Rev. Mod. Phys. 46 (1974) 129

[11] H. Niehus, W. Heiland, and E. Taglauer, Surf. Sci. Rep. 17 (1993) 213

[12] H. Winter, Phys. Rep. 367 (2002) 387

[13] A. W. Kleyn and T. C. M. Horn, Phys. Rev. Rep. 199 (1991) 191

[14] A. Schüller, S. Wethekam, and H. Winter, Phys. Rev. Lett. 98 (2007) 016103.

[15] P. Rousseau, H. Khemliche, A. G. Borisov, and P. Roncin, Phys. Rev. Lett. 98 (2007) 016104.

[16] A. Schüller and H. Winter, Phys. Rev. Lett. 100 (2008) 097602.

[17] D. Farias and K. H. Rieder, Rep. Prog. Phys. 61 (1998) 1575.

[18] T.K. Todorova, M. Sierka, J. Sauer, S. Kaya, J. Weissenrieder, J.-L. Lu, H.-J. Gao, S. Shaikhutdinov and H.-J. Freund, Phys. Rev. B 73 (2006) 165414

[19] J. D. O´Connor and J. P. Biersack, Nucl. Instrum. Meth. B 15 (1986) 14.

[20] J. R. Manson, H. Khemliche, and P Roncin, Phys. Rev. B 78 (2008) 155408.

[21] A. Schüller, M. Busch, S. Wethekam, and H. Winter, Phys. Rev. Lett. 102 (2009) 017602.

[22] U. Garibaldi, A. C. Levi, R. Spadacini, and G. E. Tommei, Surf. Sci. 48 (1975) 649.

[23] R. Masel, R. Merill, and W. Miller, J. Chem. Phys. 65 (1976) 2690.

[24] A. Schüller, M. Busch, J. Seifert, S. Wethekam, H. Winter, and K. Gärtner, Phys. Rev. B 79 (2009) 235425.

[25] P. Blonski, A. Kienja, and J. Hafner, Surf. Sci. 590 (2005) 88.